T cell receptor/CD3 complex internalization following activation of a cytolytic T cell clone: Evidence for a protein kinase C-independent staurosprine-sensitive step

ARTICLE *in* EUROPEAN JOURNAL OF IMMUNOLOGY · JULY 1991

Impact Factor: 4.03 · DOI: 10.1002/eji.1830210707 · Source: PubMed

8 AUTHORS, INCLUDING:

Nathalie Auphan-Anezin
Centre d'Immunologie de Marseille-Luminy
45 PUBLICATIONS **2,560** CITATIONS
SEE PROFILE

Hubert Reggio
Université de Montpellier
55 PUBLICATIONS **3,653** CITATIONS
SEE PROFILE

Anne-Marie Schmitt-Verhulst
Aix-Marseille Université
168 PUBLICATIONS **6,251** CITATIONS
SEE PROFILE

Claude Boyer[○], **Nathalie Auphan**[+○], **Frédéric Luton**[+○], **Jean-Marc Malburet**[+○], **Marc Barad**[○], **Jean-Pierre Bizozzero**[□], **Hubert Reggio**[□] and **Anne-Marie Schmitt-Verhulst**[○]

Centre d'Immunologie INSERM-CNRS de Marseille-Luminy[○] **and Laboratoire de Biologie de la Différenciation Cellulaire**[□], **Marseille**

T cell receptor/CD3 complex internalization following activation of a cytolytic T cell clone: evidence for a protein kinase C-independent staurosporine-sensitive step*

The fate of the T cell receptor (TcR)/CD3 complex was examined on a cytotoxic T lymphocyte (CTL) clone (KB5.C20) activated either via binding of an anti-TcR monoclonal antibody (mAb) or by a Ca^{2+} ionophore and phorbol 12-myristate 13-acetate (PMA). After binding of the anti-TcR mAb, electron microscopy revealed internalization through coated vesicles followed by slow degradation of the antibody as shown by use of radiolabeled mAb. The influence of activation on TcR/CD3 internalization was analyzed. The Ca^{2+} ionophore alone had no effect on internalization, whereas PMA induced an accelerated internalization of anti-TcR mAb. PMA-induced internalization was dependent on protein kinase C (PKC) as shown by its absence in PKC-depleted cells or in the presence of the PKC inhibitor staurosporine. Anti-TcR mAb-induced internalization was maintained in PKC-depleted cells, but unexpectedly remained sensitive to inhibition by staurosporine. The monovalent anti-TcR mAb Fab fragment is non-stimulatory for the CTL. It was poorly internalized but its internalization was induced by PMA. Surprisingly, on PKC-depleted cells, the Fab was internalized more readily than in untreated cells and this internalization was sensitive to inhibition by staurosporine. Inhibition of PMA-induced phosphorylation of γ and ε subunits of CD3 was demonstrated after depletion of PKC or in the presence of staurosporine, confirming that PKC function was inhibited in those conditions. Cross-linking of the TcR via plastic-coated anti-TcR mAb led to phosphorylation of CD3 γ and ε and also of ζ, known to be phosphorylated on tyrosines. All of these phosphorylation events were inhibited by treatment with staurosporine. Our results indicate that staurosporine inhibits the receptor internalization induced by anti-TcR mAb by means other than inhibition of PKC, suggesting that other kinases may control a step of this internalization process.

1 Introduction

The specificity of CTL-target cell interactions is inherent in the TcR α and β chains, whereas intracellular activation events are probably transduced by the associated CD3 molecules. Thus, the CD3 γ, δ and ε chains as well as the associated ζ-ζ and ζ-η heterodimers, although devoid of any known enzymatic activity, are thought to be connected to two distinct signaling systems, one involving phosphoinositide breakdown [1] leading to activation of PKC [2] and the other to activation of a protein tyrosine kinase [3, 4]. As a result of TcR/CD3 triggering, induced phosphorylation is observed on serine residues of the CD3 γ and ε and on tyrosine residues of the ζ chains [3, 5, 6]. To evaluate components controlling the dynamics of the TcR/CD3 complex, which may be related to the dynamics of cell-cell interactions, we analyzed the signals involved in modulation of the complex from the cell surface in comparison with those controlling CD3 phosphorylation and activation of cytolysis.

For many receptors activation by a ligand is rapidly followed by internalization of the receptor ligand. For some membrane proteins internalization is constitutive and may depend on the association of adaptor proteins of the coated vesicles with aromatic amino acid residues in the cytoplasmic domain of the receptor [7]. The role of receptor internalization may be distinct for each receptor: entry of nutrient inside the cell for the transferrin receptor [8, 9], intracellular signaling or down-regulation as for the epidermal growth factor (EGF) [10] or IL 2 [11] receptors. Often conditions which induce phosphorylation of the receptor also lead to internalization [12], as it is the case for the TcR/CD3 receptor on T cells [13–15]. In the work presented here, the effects of different TcR ligands and protein kinase inhibitors were analyzed on TcR/CD3 internalization and CD3 phosphorylation in a CTL clone. The results suggest that a staurosporine-sensitive protein kinase, distinct from PKC may control TcR/CD3 complex sequestration.

[I 9089]

* This work was supported by institutional grants from the Institut National de la Santé et de la Recherche Médicale, the Centre National de la Recherche Scientifique and the Association pour la Recherche sur le Cancer.

+ Predoctoral fellowships from the Ministère de la Recherche et de la Technologie.

Correspondence: Anne-Marie Schmitt-Verhulst, Centre d'Immunologie INSERM-CNRS de Marseille-Luminy, Case 906, F-13288 Marseille Cedex 9, France

Abbreviations: **MBV:** Multivesicular bodies **EGF:** Epidermal growth factor **$[Ca^{2+}]_i$:** Intracellular Ca^{2+} concentration **MRFI:** Mean relative fluorescence intensity

0014-2980/91/0707-1623$3.50+.25/0

2 Materials and methods

2.1 Cells and reagents

KB5.C20 is a CTL clone of B10.BR origin specific for the H-2K^b alloantigen, which is maintained in long-term culture as already described [16]. The protein kinase inhibitors H-7, H-8 and staurosporine (Calbiochem, La Jolla, CA) were diluted in water for H-7 and H-8 and in DMSO for staurosporine. PMA (Sigma, St. Louis, MO) was used from a stock solution at 1 mg/ml ethanol and ionomycin (Calbiochem) from a 5 mM solution in DMSO.

2.2 Antibodies

The mAb Désiré-1 is a mouse IgG$_{2a}$ specific for the TcR of clone KB5.C20 [17]. The Fab fragment was prepared as previously described [18]. mAb 145.2C11, a hamster IgG specific for mouse CD3(ε) [19] was a gift from O. Leo and J. Bluestone (Chicago, IL). H-2K^k-specific mAb 100.30.33, a mouse IgG$_{2b}$ [20] was obtained from G. Hämmerling, Heidelberg, FRG. Each of the mAb was purified on protein A-Sepharose as previously described [17].

2.3 Electron microscopic analysis

Cells were incubated with anti-TcR or with anti-H-2K^k mAb at 10 μg/ml for 1 h on ice with occasional shaking, washed three times with RPMI containing 10% FCS, followed by an incubation with protein A-gold (mean diameter 10 nm; Janssen Life Sciences Products, Beerse, Belgium) for 1 h on ice; the cells were washed three more times and were either kept at 0 °C as controls or at 37 °C for different periods of time. Cells were then fixed with 2% glutaraldehyde (Ladd, Burlington, VT) in a 0.05 M sodium cacodylate buffer, pH 7.2, 50 mM KCl, 2.5 mM $MgCl_2$, 1.25 mM $CaCl_2$, postfixed with 1% OsO_4 in PBS, stained in block in Mg, uranyl acetate, dehydrated in graded ethanol and embedded in Epon (Polaron). Sections were stained with lead and uranyl acetate and observed on a Hitachi (Tokyo, Japan) EM600 electron microscope.

2.4 Labeling of mAb with FITC

FITC (Sigma) diluted in DMSO (1 mg/ml) was added (100 μg FITC/mg protein) to mAb in 0.1 M $NaHCO_3$ (pH 7.8); the solution was mixed and incubated for 2 h at 37 °C, then filtered through a Sephadex G-25 column and centrifuged (20 min, 25 psi) using a Beckman (Palo Alto, CA) airfuge.

2.5 Analysis of internalization and ligand degradation using ^{125}I-labeled mAb

The general protocol is outlined in Fig. 3 A. KB5.C20 cells were incubated with ^{125}I-labeled mAb (4×10^5 cpm/10^6 cells/0.05 ml) at 0 °C for 2 h, washed three times with RPMI containing 10% FCS and further incubated as duplicate aliquots of 5×10^5 cells/0.2 ml at 0 °C for the controls or at 37 °C for the experimental groups. After various times of incubation cells were centrifuged after addition of 0.8 ml medium to each sample; supernatants (SN1) were saved. Cell pellets (pellet$_2$) were treated with 0.5 ml acid solution (0.15 M acetic acid, 0.15 M NaCl) for 3 min on ice and 0.5 ml FCS were added before centrifugation. Supernatants (SN2) were collected and the cell pellets (pellet$_3$) washed once with RPMI 10% FCS. After centrifugation the supernatants (SN3) were pooled with the acid wash (SN2) and cpm were counted in each sample (pellet$_4$ and SN2 + SN3). Cell viability was verified (80%–90% viable cells).

For internalization measurements, the percentages of internalized mAb were calculated with respect to the amount of mAb bound at any time point as follows: (acid resistant cpm in pellet$_4$)/[pellet$_4$ + (SN2 + SN3)] × 100.

To evaluate the proportion of fully degraded mAb, cpm precipitated by 12.5% final concentration of trichloroacetic acid (TCA) for 30 min at 0 °C in each SN1 were determined and expressed as % of the total cpm in the corresponding SN1.

Evaluation of partial degradation of ^{125}I-labeled mAb was performed by SDS acrylamide (12.5%) gel electrophoresis [21] after solubiliziation of each acid resistant cell pellet (pellet$_4$) followed by autoradiography. The gels were scanned (GS300 scanning densitometer, Hoefer Scientific Instruments, San Francisco, CA) at the positions of the IgG$_{2a}$ H chain (50 kDa) and of its degradation products (33–30 kDa). The percentage of degradation of the IgG$_{2a}$ H chain (50 kDa) was calculated as: A of 33–30 kDa fragments/[A of H chain (50 kDa) + A of 33–30 kDa fragments] × 100.

2.6 Measure of receptor modulation using fluorescent mAb

Modulation was induced during incubation of cells either in medium as control, or with different inducing agents. mAb were used either in soluble form (30 μg/ml) or plastic-coated [a 10 μg/ml solution was used for the coating of tissue culture plates (24 well Costar, Oxnard, CA)]. After incubation, cells were washed twice in PBS containing 0.5% FCS and distribution in a U-bottom microculture plate at 2×10^5 cells/well for fluorescence staining. After centrifugation of the plates, 50 μl of a saturating concentration of fluorescent mAb was added. After 45 min on ice, the cells were washed twice in PBS/FCS, were resuspended in PBS containing 1 mM EDTA and were fixed by transfer to a tube containing the same volume of 2% formaldehyde before being analyzed (5000 cells/sample) on an ODAM (Wissemburg, France) model ATC cytofluorimeter.

Figure 1. Electron micrographs showing entry of TcR into ▶ KB5.C20 cells. Entry of the TcR was monitored using mAb Désiré-1 followed by protein A-gold. (a) Surface labeling at 0 °C. After 5 (b) and 10 (c) min at 37 °C, some labeling was observed in coated pits and coated vesicles. As early as 10 min, some labeling was observed in multivesicular bodies (MVB) (d). After 90 min (e) and 3 h (f) at 37 °C, the label was often found in vesicles which could be part of an endocytic and/or of a recycling pathway. The cisternae of the Golgi complex (GC) were never labeled. (a) × 30 000; (b) × 1 000 000; (c) × 80 000; (d–f) × 40 000.

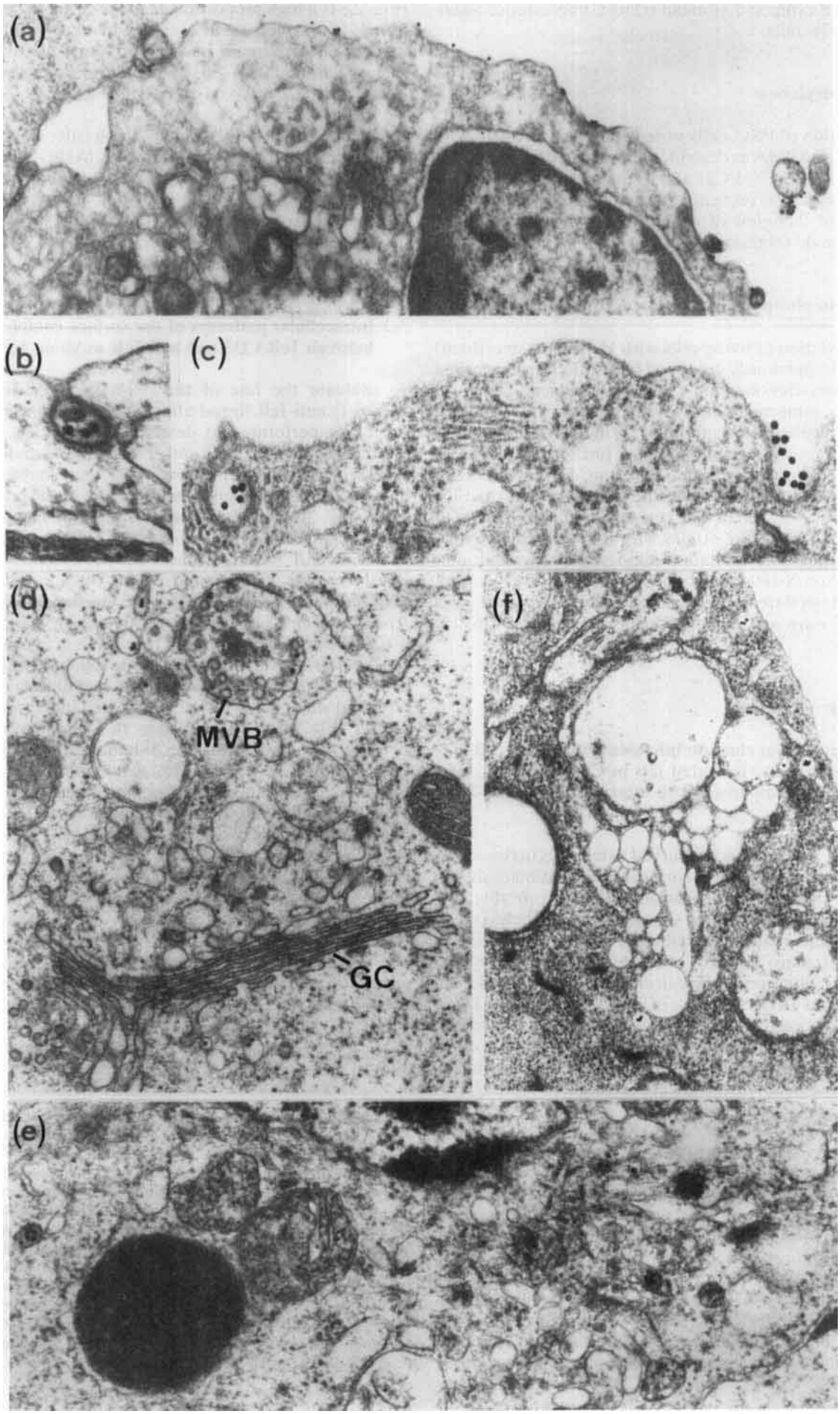
(a)
(b)
(c)
(d)
MVB
GC
(f)
(e)

Results are expressed as mean relative fluorescence intensity (MRFI) units.

2.7 PKC depletion

For depletion of PKC, cells were incubated overnight with 0.5–1.0 μg/ml PMA as described [22], washed three times in medium (RPMI-5% FCS) at 0 °C and, when indicated, *de novo* synthesis was prevented during further incubation by addition of 20 μg/ml of the protein synthesis inhibitor cycloheximide (Sigma).

2.8 Protein phosphorylation

Phosphorylation of living cells with $H_3{}^{32}PO_4$ (Amersham) was done as previously described [23]. Briefly, cells washed in phosphate-free medium were first incubated 30 min at 37 °C in the same medium, followed by a centrifugation and a further incubation 30 min at 37 °C in the same medium, followed by a centrifugation and a further incubation at 37 °C for 3 h in the presence of 0.5 mCi $H_3{}^{32}PO_4/2 \times 10^7$ cells/ml. After centrifugation, the cells were activated for 20–45 min at 37 °C in the presence of the indicated activators, washed three times with PBS containing phosphate and protease inhibitors and lysed in 1% digitonin, 0.12% Triton X-100 [24] in the same buffer. Lysates were immunoprecipitated and analyzed on acrylamide gels under reducing conditions as previously described [6, 17, 21, 23].

3 Results

3.1 Evidence from electron microscopy for TcR/CD3 internalization via coated pits in CTL clone KB5.C20: comparison with internalization of H-2 molecules

Using protein A-gold, we observed complexes between the TcR and the mAb Désiré-1 during internalization as shown in Fig. 1. Shortly after incubation at 37 °C (5 min: Fig. 1b; 10 min: Fig. 1c), grains were seen in pits and vesicles (some of which were coated, as well as in multivesicular bodies (MVB) (10 min: Fig. 1d). At later times (up to 3 h; Fig. 1e, f), grains were visible in endosomes and MVB. This is consistent with the slow rate of entry of the TcR/CD3 (see following sections). As a comparison, the internalization of the H-2K^k molecule was analyzed in the same cells using mAb 100.30.33 and protein A-gold (Fig. 2). Stronger labeling was observed, which reflects the high level of H-2K^k expression on KB5.C20 cells [23].

Grains were seen first in coated vesicles (Fig. 2b, c), followed by their engagement in tubular structures (Fig. 2d–f), which may belong to the early endosomal system. After 90 min of incubation the grains appeared to accumulate in MVB (Fig. 2h, i). Connections between the tubular structures and larger vesicles were occasionally observed (Fig. 2f), possibly reflecting a continuous endosomal system [25]. Continuity between tubules and the plasma membrane was also occasionally observed (Fig. 2d), but there is no evidence that this constitutes a mechanism of entry into the cell. At later time periods (Fig. 2g–i) a high proportion of the H-2 molecules was still found at the cell surface, in agreement with previous reports on the small fraction of internalized H-2 [26] (plateau around 25%–30% internalization of the surface-bound anti-H-2 mAb on KB5.C20 cells [23]).

In conclusion, both TcR and H-2 molecules were internalized. Differences appeared, however, in their intracellular distribution. H-2 molecules more often appeared in tubular structures (Fig. 2f–h). The question as to whether this corresponds to a different internalization pathway or to the quantitative differences in the expression of the two molecules remains to be analyzed.

3.2 Intracellular pathways of the surface complexes between TcR/CD3 and anti-TcR mAb on KB5.C20

To evaluate the fate of the ^{125}I-labeled Désiré-1 (^{125}I-Désiré-1) anti-TcR ligand after internalization, an experiment was performed as described in Fig. 3A, in which internalization (Fig. 3B) and ^{125}I-labeled ligand degradation were followed by measure ot TCA-precipitable cpm in SN (Fig. 3C) and gel analyses of the size of the internalized mAb (Fig. 3D) as a function of time of incubation in the absence or in the presence of NH_4Cl. In the presence of 10 mM NH_4Cl, which increases the pH of endosomes and lysosomes, the kinetics and extent of internalization of ^{125}I-Désiré-1 anti-TcR mAb were unchanged (Fig. 3B). Analyses of cpm in SN indicated that during incubations at 0 °C 80% of the cpm were TCA precipitable, as compared to 70% and 60% after incubation of the cells at 37 °C for 2–8 h and for 20 h, respectively. This degradation was not observed when the cells were incubated in the presence of NH_4Cl (Fig. 3C). To appreciate the degradation of the ^{125}I-Désiré-1 mAb during the 20-h incubation at 37 °C, cell lysates were analyzed by SDS acrylamide gels. Densitometric analyses of the gel autoradiographies are reported in Fig. 3D. Starting at 90 min of incubation at 37 °C, degradation of the H chain of the ^{125}I-Désiré-1 IgG_{2a} into a 33-kDa fragment was observed. After 5 h, a second fragment of 30 min, apparently derived from the 33-kDa fragment, was observed. At 20 h, a 12-kDa fragment derived from the H chain and a faint band at 23 kDa derived from the L chain were seen (results not shown). In the presence of NH_4Cl the degradation proceeded at a slower rate (Fig. 3D). These results are compatible with degradation in a late endosome compartment.

Figure 2. Electron micrographs showing entry of H-2K into ▶ KB5.C20 cells. Entry of H-2K was monitored with mAb 100.30.33 followed by protein A-gold. (a) Surface labeling at 0 °C. After 5 min at 37 °C (b–d), the labeling was observed in some coated pits and coated vesicles (b, c). Occasionally label was observed in invaginations of the plasma membrane (d), possibly due to multiple binding of gold particles to H-2K molecules. As early as 10 min at 37 °C, the label was seen in the tubulovesicular system (arrow) of the early endosomal system (e, f). At 90 min (g–i), the tracer accumulated in late endosomes and in multivesicular bodies (MVB) (i), but was still observed in the tubular system near the plasma membrane (g, h). At any time point there was still surface labeling, occasionally interacting with shed membranes. (a) × 30000; (b–e) × 40000; (f–i) × 30000.

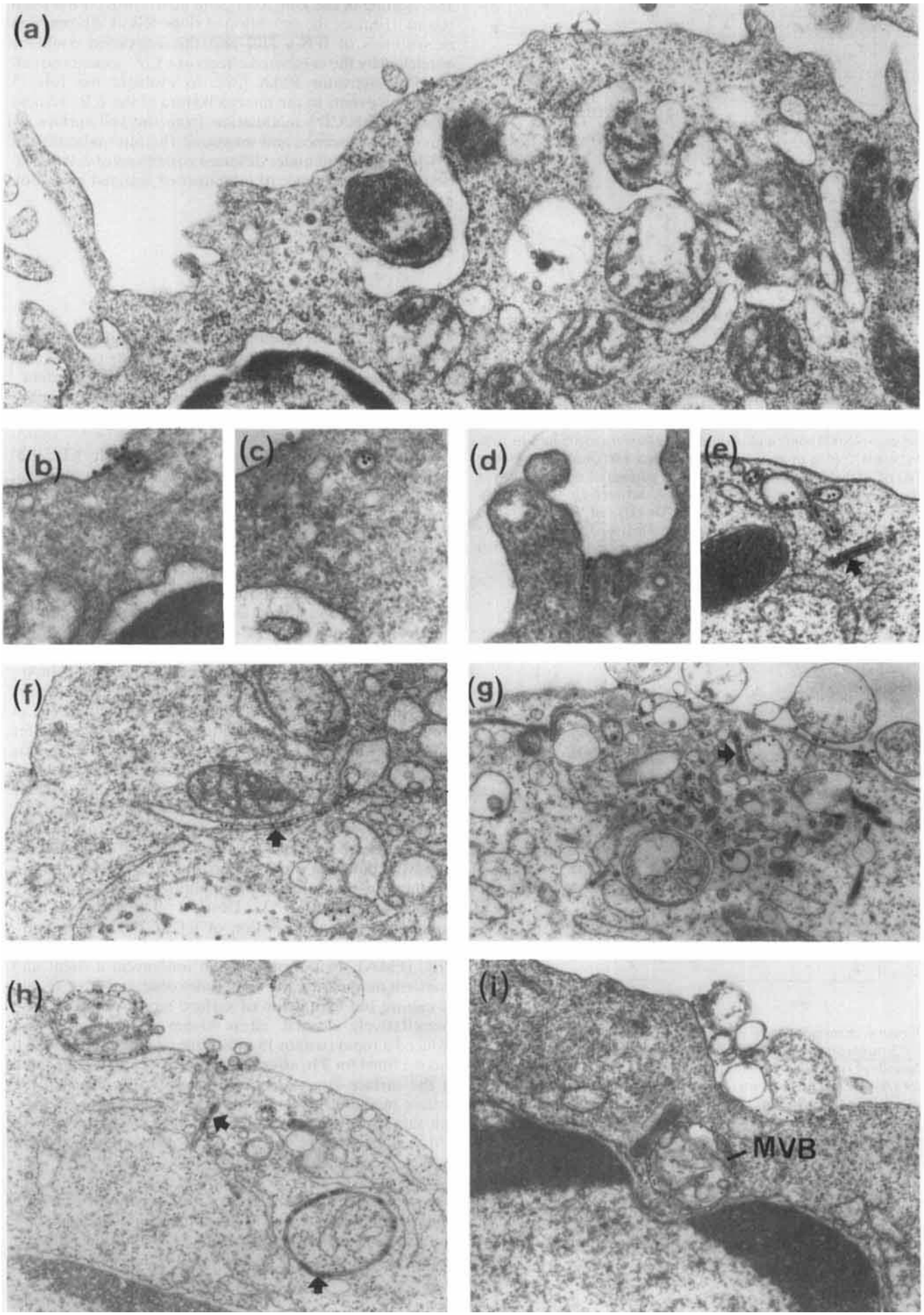
(a)
(b)
(c)
(d)
(e)
(f)
(g)
(h)
(i)
MVB

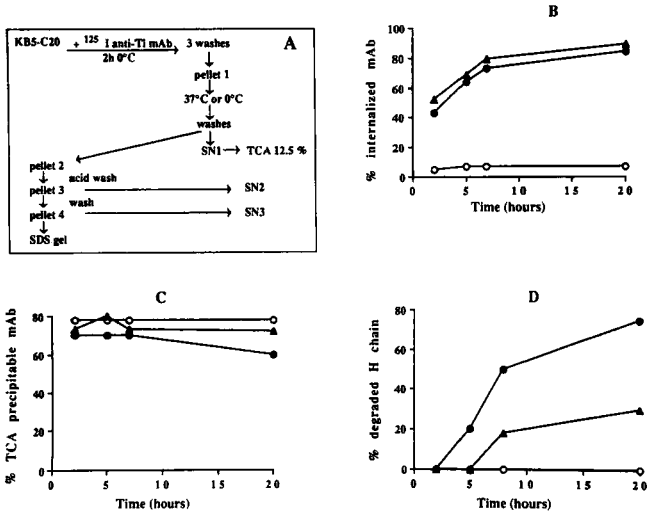

Figure 3. Experimental scheme and measurements of ^{125}I-labeled anti-TcR (^{125}I-mAb) internalization and degradation. (A) As described in Sect. 2.6, KB5.C20 cells incubated with ^{125}I-labeled anti-TcR mAB Désiré-1 (anti-Ti) for 2 h at 0 °C were washed (cell pellet$_1$ = 45 000 cpm) and aliquots of cells were incubated in 10% FCS at 0 °C (○), or at 37 °C in the absence (●) or in the presence (▲) of 10 mM NH_4Cl for the indicated periods of time. Following the treatments described in Sect. 2.6 outlined in scheme (A), percentages, of internalized ^{125}I-mAb (B), of fully degraded ^{125}I-mAb (C) and of partial degradation (to 33–30 kDa) of the 50-kDa H chain of ^{125}I-mAb Désiré-1 were measured as described (Sect. 2.6).

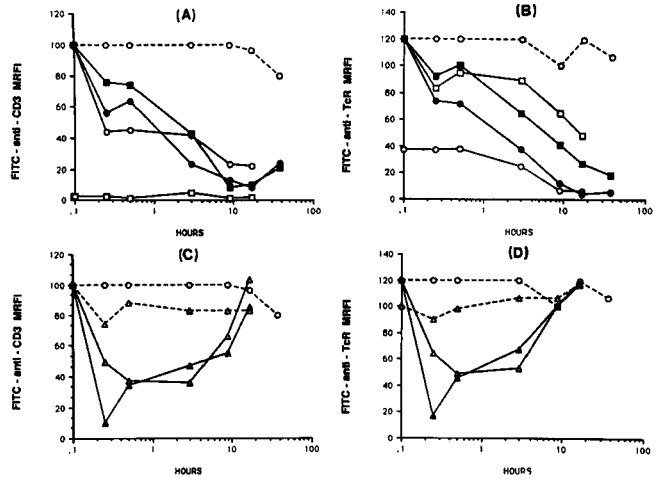

Figure 4. Kinetics of the cell surface modulation of the TcR and CD3 molecules. KB5.C20 cells were incubated for the indicated periods of time at 37 °C in the following conditions (see Sect. 2.7); for (A) and (B): in medium (RPMI 5% FCS) without addition (○, stippled lines), with anti-CD3 ε mAb 145.2C11 in soluble (□) or plastic-coated (■) form, with anti-TcR mAb Désiré-1 in soluble (○) or plastic-coated (●) form; for (C) and (D): in medium without addition (○, stippled lines), with 30 ng/ml PMA (▲), with 4 μM ionomycin (△,. stippled lines), or with both (△). Staining was with FITC-labeled anti-CD3 mAb 145.2C11 (A, C) or FITC-labeled anti-TcR mAb Désiré-1 (B, D). Results are expressed as MRFI units as a function of time. The first point of the logarithmic time scale (0.1) corresponds to cells labeled before any incubation (time 0).

The binding of the anti-TcR ligand mAb Désiré-1 has been shown to induce the activation of clone KB5.C20, resulting in synthesis of IFN-γ [18] and this activation could be mimicked by the combined effects of a Ca^{2+} ionophore and the PKC-activator PMA [27]. To evaluate the role of activation events in the internalization of the TcR, we next analyzed TcR/CD3 modulation from the cell surface by immunofluorescence and measured the internalization of ^{125}I-labeled ligand under different conditions of cell activation or in the presence of inhibitors of selected activation pathways.

3.3 Kinetics of the modulation of the TcR/CD3 complex induced by anti-TcR, anti-CD3 or agents causing an increase in the intracellular free Ca^{2+} concentration or an activation of PKC as measured by fluorescence analysis

Since binding of anti-TcR α/β mAb Désiré-1 to KB5.C20 does not affect binding of FITC-anti-CD3 ε mAb 145.2C11 and *vice versa*, staining with FITC-145.2C11 was performed to measure modulation induced by mAb Désiré-1 (Fig. 4A) and reciprocally (Fig. 4B). Data in Fig. 4A indicate that KB5.C20 cells, incubated with anti-TcR mb Désiré-1 at 37 °C, showed a 60% reduction in expression of CD3 after 15 min and 90% reduction after a 20-h incubation. When soluble anti-CD3 mAb was used for incubation, no staining was detected using the FITC-anti-CD3, due to competition for binding of unlabeled and labeled mAb. This was not the case for cells incubated with plastic-coated anti-CD3 mAb. The latter could be observed to modulate the expression of CD3 with kinetics similar to those seen in the presence of anti-TcR mAb, soluble or plastic-coated. In Fig. 4B, after staining with FITC-Désiré-1, a reduction in binding was observed on KB5.C20 cells incubated with soluble or coated anti-CD3. The modulation appeared less drastic (40% after 15 min), but was also maximal after a 20-h incubation (70% for soluble and 90% for coated anti-CD3). The incubation with the unlabeled Désiré-1 mAb only led to partial blocking of binding of the FITC-labeled mAb. Modulation measured by staining with FITC-145.2C11 (Fig. 4C) and with FITC-Désiré-1 (Fig. 4D) was also monitored during incubation of KB5.C20 cells in conditions which increase $[Ca^{2+}]_i$ (ionomycin) or an activation of PKC (PMA). In the presence of ionomycin a slight and transient modulation was sometimes observed after 15 min of culture but expression of surface receptors was always quantitatively normal after 30 min of culture. PMA induced a rapid (within 15 min) surface modulation, which was maximal for 2 h, after which time receptors reappeared at the surface even though PMA was still present in the culture medium. In the presence of ionomycin plus PMA, the same kinetics of modulation were observed as with PMA alone, except for a slightly stronger reduction in surface receptors after 15 min.

The question of a possible role of PKC in induced TcR/CD3 modulation was analyzed in experiments of PKC depletion from the cells as well as by use of PKC and other protein kinase inhibitors.

3.4 Role of PKC depletion and of protein kinase inhibitors on the TcR/CD3 modulation measured by fluorescence

The modulation of the TcR/CD3 complex was next analyzed on normal or on PKC-depleted KB5.C20 cells. As previously described in other systems [22], pretreatment of cells with a high concentration of PMA results in the degradation of PKC, and loss of kinase activity (see Sect. 3.7). As indicated in Fig. 5, where the level of FITC-145.2C11 fluorescence is represented, PKC-depleted KB5.C20 cells expressed the same level of CD3 as untreated cells. Subsequent treatment with PMA for 1 h reduced from 90 to 20 (75% modulation) the MRFI of normal KB5.C20 cells, but did not affect significantly the fluorescence of PKC-depleted cells. In contrast, treatment with the Désiré-1 mAb for 1 h reduced by 40% the MRFI on both normal and PKC-depleted KB5.C20 cells (Fig. 5A and B). Thus, in conditions of PKC depletion by PMA pretreatment, TcR/CD3 modulation was still observed after binding of anti-TcR mAb, although it could not be induced by PMA. Although distinct PKC isoenzymes could be differently affected by the PMA pretreatment [28], the PKC-depleted KB5.C20 cells used here were deficient in TcR-mediated activation for killing (results not shown) and selectively for PKC-dependent IFN-γ production [29], as well as for PMA-induced CD3γ phosphorylation (see Sect. 3.7, Fig. 8) and, therefore, appeared depleted of functional PKC.

The effects of two protein kinase inhibitors on the modulation of TcR/CD3 complexes were analyzed next. H-7 is an inhibitor of both PKC ($K_i = 6$ μM) and cAMP-dependent protein kinases ($K_i = 3$ μM) [30] and H-8 is an inhibitor of cGMP-($K_i = 0.48$ μM)- and cAMP-($K_i = 1.2$ μM)-dependent protein kinases, and is less potent in inhibition of PKC ($K_i = 15$ μM) [30]. Data indicate (results not shown) that PMA-induced modulation of TcR/CD3 was more sensitive than anti-TcR-induced modulation to the protein kinase inhibitor H-7. However, the effect of H-7 was only partial at 200 μM, the highest concentration at which H-7 could be used for reasons of cell viability. H-8 (up to 200 μM) was not inhibitory for either ligand- or PMA-induced TcR modulation (results not shown). Treatment of cells with staurosporine, described as a more selective and potent inhibitor of PKC ($K_i = 2.7$ nM) [31], caused an artifact in fluorescence measurements such that the number of receptors appeared lower on treated than on untreated cells (results not shown). Since this phenomenon was observed for every cell surface molecule tested by fluorescence measurements on KB5.C20 cells (H-2K and CD8, results not shown), another approach was used to analyze the effects of staurosporine on the dynamics of TcR/CD3 (see Sect. 3.6). Additionally, we compared internalization of the cell-activating divalent anti-TcR with that of the non-activating monovalent Fab.

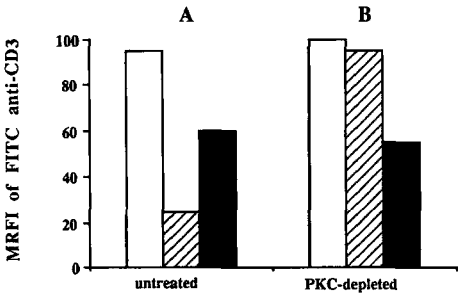

Figure 5. Analysis of TcR/CD3 modulation on PKC-depleted KB5.C20 cells. KB5.C20 cells were harvested from an overnight culture in the absence [(A) = untreated KB5.C20] or in the presence (B) = proliferation-depleted KB5.C20] of 1 μg/ml PMA as described in Sect. 2.8. Washed cells were recultured for 1 h at 37 °C with medium (□), or with 30 ng/ml PMA (▨), or with 30 μg/ml anti-TcR mAb Désiré-1 (■). After washing, cells were stained with FITC-labeled anti-CD3 ε mAb 145.2C11 and analyzed at the cytofluorimeter. Results are expressed as MRFI units.

3.5 Analysis of monovalent and divalent TcR ligand internalization using ^{125}I-labeled anti-TcR mAb and its Fab

The anti-TcR mAb Désiré-1 is an IgG_{2a} which through its two binding sites for the α/β chains of the TcR cross-links two TcR molecules and induces an activation signal as measured by IFN-γ production [18] which is PKC dependent [29]. Binding of the monovalent Fab fragment of Désiré-1 is non-stimulatory [18]. In the experiment presented in Fig. 6, KB5.C20 cells were incubated at 0 °C with ^{125}I-Désiré-1 as a divalent reagent or as a Fab, washed and further incubated at 37 °C in medium or with PMA for various periods of time and ligand internalization was

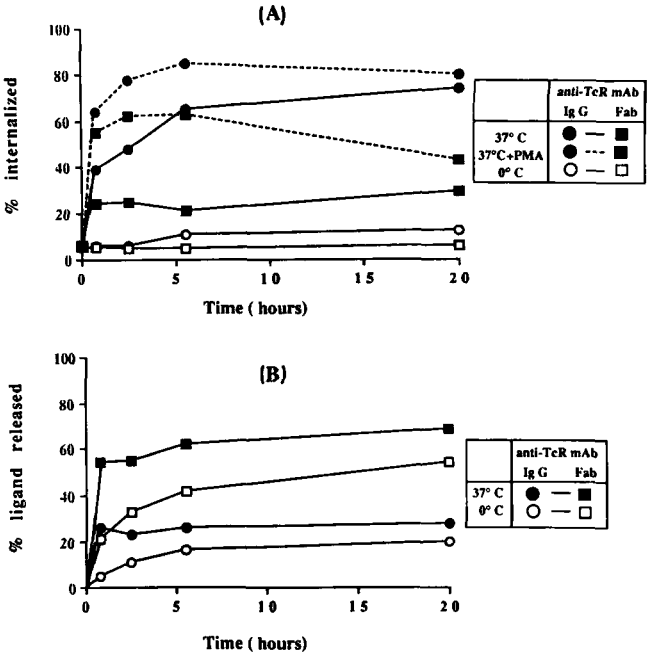

Figure 6. Characteristics of the internalization of ^{125}I-labeled anti-TcR mAb and the Fab fragment of the mAb. KB5.C20 cells were incubated with ^{125}I-labeled Désiré-1 mAb (circles) or with the ^{125}I-labeled Fab fragment of Désiré-1 mAb (squares) at 0 °C for 1 h. After washes, both samples were resuspended in RPMI 10% FCS and left at 0 °C (empty symbols) or cultured for various periods of time at 37 °C (full symbols) in medium alone (full lines) or in the presence of 30 ng/ml PMA (stippled lines). Ligand internalization, measured as described in Sect. 2.6 after acid treatment of cell-bound ligand, is expressed in (A) as the %, at any given time, of cell-bound ligand which was acid wash resistant. In (B), the % of the initially cell-bound ligand (40 000 cpm for mAb Désiré-1; 55 000 cpm for the Fab of Désiré-1) which was released during incubation is expressed as a function of time.

measured (see Sect. 2.6 and legend to Fig. 3). In Fig. 6A, it is observed that at 45 min the percentage of internalized Fab has reached a plateau at 25%, whereas the internalization of the divalent mAb (40%) continues to reach 65% at 5 h and then remains more or less constant until 20 h (70% internalized). In the presence of PMA, the internalization of the Fab is induced to 60% after 2.5 h, but does not increase further after that time. This may be correlated with the results of PMA-induced modulation (Fig. 4C and D), which is no longer efficient after 3 h of incubation. Although the dissociation rate (Fig. 6B) of the Fab (55% ligand released after 45 min at 37 °C) is greater than that of the divalent mAb (around 20% ligand released after 45 min at 37 °C), this is corrected for in the evaluation of the percentage of ligand internalization which is calculated with respect to bound ligand at any time point (see Sect. 2.6 and legend to Fig. 3B). The data suggest that the extent of ligand internalization is dependent on the extent of the activation induced by the ligand. To evaluate whether differences in PKC activation could account for these differences in internalization, PKC-depleted cells as well as the efficient PKC inhibitor staurosporine was used.

3.6 Effect of staurosporine on TcR/CD3 internalization measured with ^{125}I-labeled anti-TcR mAb or its Fab on untreated and on PKC-depleted cells

When KB5.C20 cells were incubated for 30 min with 100 nM staurosporine or left untreated, and subsequently incubated at 0 °C with ^{125}I-Désiré-1, the same number of cpm were bound, indicating that staurosporine did not affect cell surface expression of the TcR/CD3 (results not shown or cpm in the legend to Fig. 7). In the experiment presented in Fig. 7A, KB5.C20 cells were incubated in the cold with ^{125}I-Désiré-1 or its Fab before culture at 37 °C with or without staurosporine and measure of ligand internalization. Staurosporine inhibited > 50% of the internalization of ^{125}I-Désiré-1 measured in the absence (Fig. 7A) or in the presence (results not shown) of PMA. Interestingly, in the presence of the PKC inhibitor staurosporine, the internalization of the divalent mAb was reduced to that observed for the monovalent Fab (Fig. 7A), the latter being only minimally affected by the inhibitor. This observation suggested that the increased internalization of the divalent mAb could have resulted from a PKC-dependent activation event induced by the divalent, but not by the monovalent mAb. To test this hypothesis further, internalization of divalent and monovalent mAb was measured on PKC-depleted KB5.C20 cells by the same method.

Cycloheximide, which has no effect on internalization (results not shown) was present during incubation to prevent resynthesis of PKC. The results (Fig. 7B compared to Fig. 7A) indicate that internalization of both the anti-TcR mAb and of its Fab was increased on the PKC-depleted cells (60% at 45 min to 80% at 5 h for the divalent mAb; plateau around 40% for the Fab), but no further PMA-induced internalizations were observed (dotted lines superimposed on full lines in Fig. 7B), consistent with the PKC depletion of the cells. Surprisingly, however, staurosporine strongly inhibited the internalization of both divalent and monovalent ligands on the PKC-depleted cells [from 78% to 43% for the divalent mAb; from 40% to 20% for the Fab (Fig. 7B)]. The latter results suggest that staurosporine may

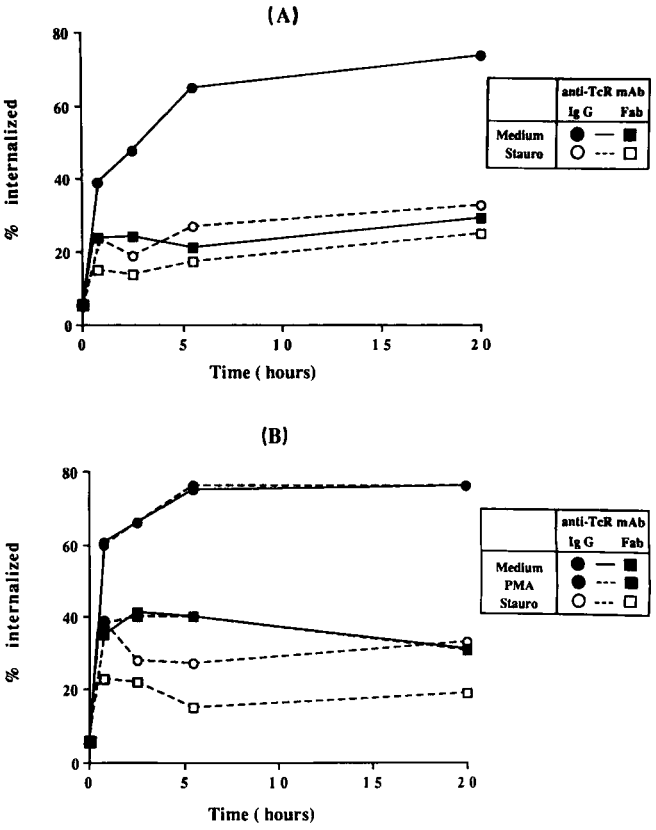

Figure 7. Differential effects of staurosporine on internalization of the anti-TcR mAb or its Fab on untreated and on PKC-depleted KB5.C20 cells. Untreated and PKC-depleted (see Sect. 2.8) KB5.C20 cells were incubated with ^{125}I-labeled Désiré-1 mAb (circles) or with the ^{125}I-labeled Fab fragment of Désiré-1 mAb (squares) at 0 °C for 1 h. Washed cells were resuspended in RPMI 10% FCS with addition of 20 μg/ml cycloheximide. Each sample was further incubated at 37 °C for various periods of time without further addition [full symbols, full lines in (A) and (B)], with 30 ng/ml PMA [full symbols, stippled lines in (B) only], with 100 nM staurosporine [empty symbols, stippled lines in (A) and (B)]. The % internalized mAb or Fab was determined as described in Sect. 2.5. Bound cpm were 40 000 for the ^{125}I-labeled Désiré-1 mAb and 55 000 cpm for the ^{125}I-labeled Fab on either untreated or PKC-depleted KB5.C20 cells.

have inhibitory effects other than those reported on PKC [31]. To evaluate more directly the effects of kinase inhibitors, CD3 protein phosphorylation was analyzed.

3.7 Analysis of CD3 phosphorylation after PKC depletion or kinase inhibitors

In the mouse, PMA has been shown to induce the phosphorylation of CD3 ε and CD3 γ in both CD4$^+$ helper [3, 5] and CD8$^+$ cytolytic [6, 23] T cells. A similar result is illustrated in Fig. 8 for the KB5.C20 cells. Presence of either 200 μM H-7 or 200 μM H-8 was without detectable effect on the PMA-induced phosphorylation of the CD3 ε (faint) and γ (strong) bands, indicating that H-7 cannot be used efficiently as a PKC inhibitor on the CTL. Staurosporine at 200 nM was clearly inhibitory, leading to the disappearance of the faint CD3 ε band and to a significant reduction in the intensity of the CD3 γ band (Fig. 8A). Results in Fig. 8B also show that in conditions of PKC

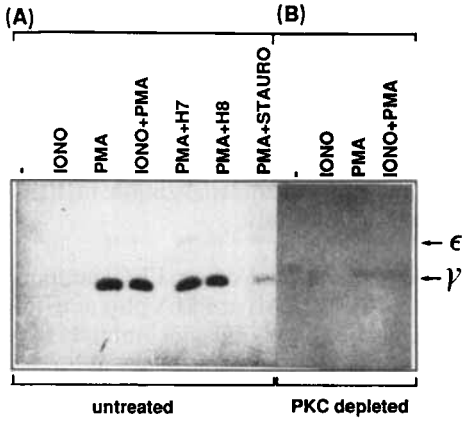

Figure 8. Inhibition of PMA-induced CD3 phosphorylation after PKC depletion or in the presence of staurosporine. Untreated (A) and PKC-depleted [see Sect. 2.8; (B)] KB5.C20 cells were incubated in ^{32}P-labeling buffer (see Sect. 2.9), washed and incubated in the presence of: medium (–); 2 μM ionomycin (iono); 30 ng/ml PMA (PMA); ionomycin and PMA (iono + PMA); 200 μM H-7 and PMA (PMA + H-7); 200 μM H-8 and PMA (PMA + H-8), or 100 nM staurosporine and PMA (PBS + STAURO) as indicated. Immunoprecipitation with CD3 ε-specific mAb 145.2C11 and 1-D 12.5% acrylamide gels were run in nonreducing conditions as described in Sect. 2.9. Arrows indicate the posisitons of the CD3 γ and CD3 ε bands.

depletion after overnight treatment with 500 ng/ml PMA, a faint band was observed for CD3 γ in non-stimulated PKC-depleted KB5.C20 cells, the intensity of which was not increased by PMA treatment. Thus, clear inhibition of PMA-induced phosphorylation of CD3 γ (and ε) was observed in the presence of staurosporine and after PKC depletion. Activation of Tcells by antigen in the presence of appropriate APC [3] or by anti-TcR mAb [6] induces the phosphorylation of CD3 γ and ε on Ser residues and the phosphorylation of the CD3-associated molecule ζ on Tyr residues [3]. Results in Fig. 9, where CD3 immunoprecipitates are analyzed in 2-D gels (reduced/nonreduced) indicate that activation of KB5.C20 cells by anti-TcR mAb induced the phosphorylation of CD3 γ and ε as well as that of the CD3-associated ζ (spot under the diagonal; Fig. 9C). The presence of 100 nM staurosporine inhibited the phosphorylation of CD3 γ and ε, as well as that of the CD3-associated ζ molecule (Fig. 9D), as indicated by the relative intensities obtained from gel scanning (Table 1).

Table 1. Quantitative evaluation of CD3 phosphorylation

	Relative intensities of ^{32}P-labeled bands of CD3 immunoprecipitates after activation with		
	CD3 γ	CD3 ε	CD3 ζ
No	1.00[a)]	1.00	1.00
PMA	3.50	1.80	0.73
Anti-TcR	3.63	2.46	1.34
Anti-TcR + staurosporine	0.96	1.45	0.86

a) The gel shown in Fig. 9 was scanned using a scanning densitometer and values were normalized to those for the non-activated sample.

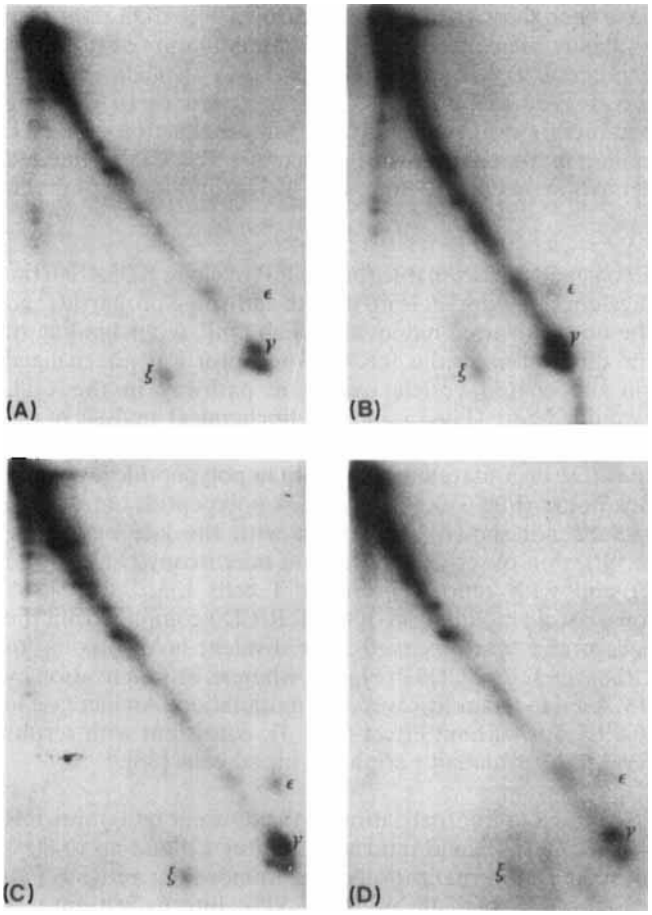

Figure 9. Effect of staurosporine on the anti-TcR-induced phosphorylation of CD3 components. After incubation in ^{32}P-labeling buffer, KB5.C20 cells were washed and incubated in medium (A), 30 ng/ml PMA (B), plastic-coated anti-TcR mAb Désiré-1 alone (C) or with 100 nM staurosporine (D). After 30 min of incubation at 37 °C, cells were washed and lysed. Immunoprecipitations were performed on each lysate using anti-CD3 ε mAb 145.2C11 and were analyzed on 2-D (horizontally in nonreduced, vertically in reduced conditions) 12.5% acrylamide gels. The positions of the CD3 γ, CD3 ε and ζ bands are indicated. Relative intensities determined by gel scanning are reported in Table 1.

The coefficient of increase in phosphorylation of ζ was low in this experiment. ζ phosphorylation induced by the anti-TcR mAb was reproducibly inhibited by staurosporine in different experiments (ratio of intensity in TcR-activated cells in the absence and in the presence of staurosporine $= 2.0 \pm 0.7$) These results suggest that in the conditions used, staurosporine inhibits not only the PKC-dependent phosphorylation of CD3 γ and ε but also the anti-TcR mAb-induced phosphorylation mediated by a Tyr kinase, known to phosphorylate the ζ molecules.

4 Discussion

For target cell lysis to be efficient, a CTL has to be able to disengage and reengage a number of times in target cell interaction. The mechanisms involved in such dynamic behavior have not been elucidated. Changes in affinity between T cell-expressed adhesion and target cell-expressed ligand molecules, such as LFA-1/ICAM which

have been shown to be under control of TcR/CD3 activation [32], may be involved. Local down-modulation of TcR/CD3 expression as a result of activation may also contribute to the disengagement. These questions led us to evaluate parameters controlling TcR/CD3 internalization in a CTL clone, in particular with respect to TcR/CD3-mediated activation events leading to CD3 protein phosphorylation.

Two ligands are available for the TcR of clone KB5.C20: the divalent IgG_{2a} anti-TcR mAb with activating properties and the non-activating monovalent Fab [18]. After binding of the divalent mAb the TcR/CD3 receptor was internalized via the coated vesicle endocytic pathway in the CTL examined here (Figs. 1 and 2). Biochemical analysis of the fate of internalized anti-TcR mAb revealed an NH_4Cl-sensitive degradation to 33–30-kDa polypeptides within a few hours (Fig. 3) and to 12-kDa polypeptides after 20 h (results not shown), consistent with the late endosome localization observed by electron microscopy (Figs. 1 and 2) and with reports in other T cells [33, 34, 35]. A long-lasting modulation of the TcR/CD3 complex from the cell surface was observed after divalent mAb binding to either the TcR or CD3 ε (Fig. 4), whereas PKC activation by PMA led to a rapidly reversible modulation. An increase in $[Ca^{2+}]_i$ was without effect (Fig. 4), consistent with results reported for human peripheral blood cells [36].

In contrast to internalization of the divalent IgG_{2a} anti-TcR mAb (= 50% ligand internalized after 1 h and up to 80% after 20 h), internalization of the monovalent anti-TcR Fab was low (a plateau of 20%–30% internalization was reached after 1 h). This difference did not result from the greater dissociation rate of the Fab (Fig. 6A and B). The possibility was considered that internalization measured with the non-activating ligand Fab corresponded to constitutive cycling [13, 14] of the TcR/CD3 complex, whereas the divalent activating ligand IgG led to CD3 γ, ε and ζ protein phosphorylation ([6] and Fig. 9) and sequestration of the complex [12]. Either PKC, involved in phosphorylation of CD3 γ and ε [3], or a tyrosine protein kinase, responsible for CD3 ζ phosphorylation [3, 4], could thus be involved in the increased intracellular retention of the ligand-receptor complex. PKC, however, does not appear to be involved in this internalization/retention, since this pathway is active even in PKC-depleted cells (Figs. 5 and 7). Although different PKC isoenzymes may exist in these Tcells [37, 38], relevant PKC was clearly inactive in the PKC-depleted cells as indicated by absence of PMA-induced phosphorylation of CD3 γ and ε (Fig. 8) and lack of PMA-dependent internalization of the TcR/CD3 complex (Figs. 5 and 7). However, we cannot exclude a residual phosphorylation of CD3 γ or ε as a result of the high-dose PMA pretreatment which may explain the increased Fab internalization in PKC-depleted, as compared to the untreated, cells (Fig. 7). A potential role for serine phosphorylation, known to occur on either Ser 123 or Ser 126 of the human CD3 γ chain [39] depending on conditions of protein kinase and phosphatase activation [40], is being further evaluated by reconstitution of CD3 γ-deficient CTL variants. For the EGF receptor, a specific Thr residue in the cytoplasmic domain of the receptor is required for PMA-induced, PKC-dependent receptor internalization, but not for ligand-induced internalization [41]. Additionally, the integrity of the EGF receptor tyrosine kinase activity seems required for degradation of the receptor which cycles without degradation when the kinase domain is mutated [42]. Samelson and colleagues [3] had shown that tyrosine phosphorylation of the ζ chain was not abolished after PKC depletion [3]. Thus, ζ chain phosphorylation or a tyrosine kinase activity associated with the TcR could be responsible for the observed ligand-induced internalization in PKC-depleted cells observed in our study.

Staurosporine, characterized as a potent PKC inhibitor [31], inhibited 50% of anti-TcR mAb or PMA plus anti-TcR mAb-induced internalization but did not inhibit Fab-induced internalization (Fig. 7). This could be an additional argument that cycling measured with the Fab is constitutive. Consistent with this hypothesis, internalization of the transferrin receptor, which is followed by receptor recycling, was not affected by staurosporine on CTL clone KB5.C20 (results not shown). As expected for a PKC inhibitor, staurosporine inhibited CD3 γ and ε, but unexpectedly also ζ protein phosphorylation induced by anti-TcR mAb (Fig. 9; Table 1). Taken together, these results suggest that staurosporine has inhibitory effects other than those on PKC function, consistent with reports in other systems [31, 43–45]. The following possibilities can be considered: (a) the staurosporine-inhibited step directly involves the tyrosine kinase activity associated with the TcR/CD3, a hypothesis compatible with the inhibition of ζ phosphorylation by staurosporine. This drug has also been found to inhibit $p60^{v\text{-}src}$ [45] and EGF receptor [46] tyrosine protein kinases; this would not explain, however, the inhibition of Fab measured internalization on PKC-depleted cells. (b) Staurosporine may affect cell surface distribution of receptors, possibly through an indirect effect on actin filaments [43]; however, cytochalasin D, known to inhibit microtubule organization [47], did not inhibit TcR/CD3 internalization (results not shown). (c) Staurosporine may inhibit a PKC- and tyrosine kinase-independent step of intracellular vesicle targeting controlled by a serine/threonine kinase as recently described in yeast mutants [48]. The latter possibility is compatible with the pattern of inhibition by staurosporine or internalization measured with either divalent or monovalent TcR ligands on PKC-depleted cells (Fig. 7A and B).

Available data suggest a sequence of three distinct steps controlling TcR/CD3 internalization/sequestration induced by anti-TcR mAb (see Fig. 10). The first step, common to receptor cycling and sequestration, involves the association with adaptor proteins in coated pits [7] which requires the presence of the appropriate aromatic residue [7] in the cytoplasmic domain of one of the CD3 components, as shown for the transferrin receptor [49], the EGF receptor [42] and HLA class I molecules [50]; this step is measured by Fab internalization and receptor cycling [13, 14]. The signal for step two is the phosphorylation of a CD3 component (CD3 γ?); this step proceeds in conditions of PKC activation by PMA or anti-TcR mAb, but not its Fab. The available means of depleting PKC by pretreatment with high concentrations of PMA appear adequate for eliminating active PKC; the treatment may, however, lead to an increased proportion of Ser-phosphorylated CD3 molecules, undetected by ^{32}P incorporation; these CD3 molecules would be at the step-two stage, required to enter step three. This last step, defined by its absence of dependence on an active PKC, combined with its sensitivity

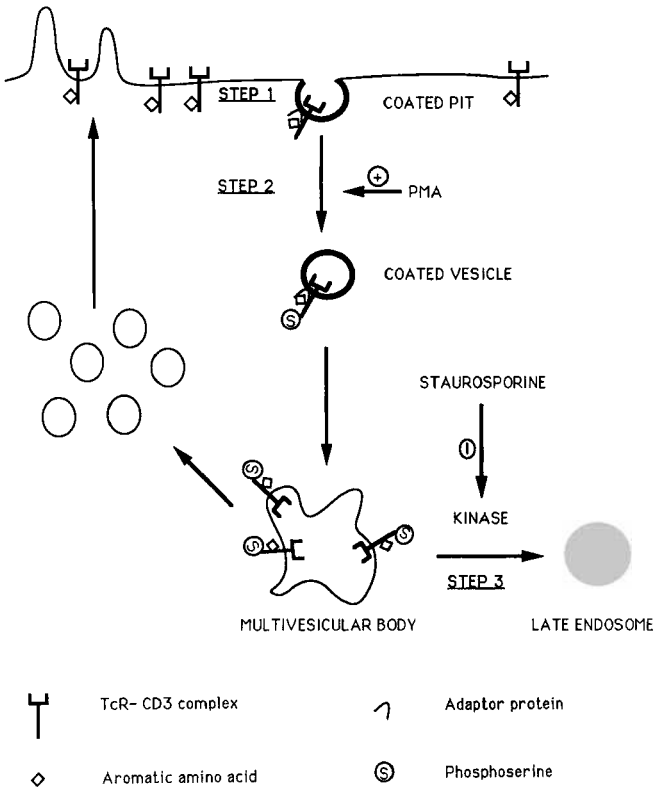

Figure 10. Proposed model for distinct steps controlling the internalization and sequestration of the TcR/CD3 complex induced by the activating divalent anti-TcR mAb.

to staurosporine, leads to a long-lasting sequestration followed by degradation of the receptor complex. It proceeds only if conditions required for steps one and two are fulfilled. All of these conditions are obtained only in the presence of the activating anti-TcR ligand (Fig. 10), leading to long-lasting sequestration, whereas PMA-induced internalization in the absence of TcR ligand may not proceed to step three, leading to short time modulation (Fig. 4). Since degradation of the Fab was not observed in KB5.C20 cells (results not shown) and no efficient and selective PKC inhibitor is yet available, these hypotheses could not be tested further at this stage. A possible role for tyrosine kinase phosphorylation of CD3 ζ and differential activation of phosphatases will also have to be evaluated.

It is difficult to know whether the fate of the TcR/CD3 complex is controlled by the activation resulting from ligand binding or additionally by the perturbation caused by the presence of the experimental ligand when one considers that its natural ligand is cell-associated MHC (and peptide), with much lower intrinsic affinity for the TcR than the experimental anti-TcR mAb ligands [18, 51]. Our approach to this question is to determine whether there is perturbation of antigen-specific cell-cell interactions in T cell variants affected in an experimentally defined pathway. In this respect, the newly defined staurosporine-sensitive, PKC-independent TcR/CD3-internalization step described here is being studied further, in particular by means of a CTL mutant which is selectively deficient in this TcR internalization pathway (F. Luton et al., unpublished results).

We thank C. Langlet, L. Leserman and P. Machy for criticism of the manuscript.

Received November 28, 1990; in revised form January 28, 1991.

5 References

1 Weiss, A., Imboden, J., Hardy, K., Manger, B., Terhorst, C. and Stobo, J., *Annu. Rev. Immunol.* 1986. *4:* 593.
2 Nishizuka, Y., *Science* 1986. *4:* 593.
3 Patel, M. P., Samelson, L. E. and Klausner, R. D., *J. Biol. Chem.* 1987. *262:* 5831.
4 Samelson, L. E., Phillips, A. F., Luong, E. T. and Klausner, R. D., *Proc. Natl. Acad. Sci. USA* 1990. *87:* 4358.
5 Samelson, L. E., Patel, M. D., Weissman, A. M., Harford, J. B. and Klausner, R. D., *Cell* 1986. *46:* 1083.
6 Boyer, C., Langlet, C., Guimezanes, A., Buferne, M., Hua, C. and Schmitt-Verhulst, A.-M., *Annu. Inst. Pasteur/Immunol.* 1987. *138:* 65.
7 Pearse, B. M. F., *EMBO J.* 1988. *7:* 3331
8 Rothenberger, S., Iacopetta, B. J. and Kühn, L. C., *Cell* 1987. *49:* 423.
9 Zerial, M., Suomalainen, M., Zanetti-Schneider, M., Schneider, C. and Garoff, H., *EMBO J.* 1987. *6:* 2661.
10 Schlessinger, J., *Biochemistry* 1988. *27:* 3119.
11 Robb, R. J. and Greene, W. C., *J. Exp. Med.* 1987. *165:* 1202.
12 Sibley, D., Benovic, J. L., Caron, M. G. and Lefkowitz, R. J., *Cell* 1987. *48:* 913.
13 Minami, Y., Samelson, L. E. and Klausner, R. D., *J. Biol. Chem.* 1987. *262:* 13342.
14 Krangel, M. S., *J. Exp. Med.* 1987. *165:* 1141.
15 Cantrell, D. A., Davies, A. A. and Crumpton, M. J., *Proc. Natl. Acad. Sci. USA* 1985. *82:* 8158.
16 Albert, F., Buferne, M., Boyer, C. and Schmitt-Verhulst, A.-M., *Immunogenetics* 1982. *16:* 533.
17 Hua, C., Boyer, C., Buferne, M. and Schmitt-Verhulst, A.-M., *J. Immunol.* 1986. *136:* 1937.
18 Hua, C., Boyer, C., Guimezanes, A., Albert, F. and Schmitt-Verhulst, A.-M., *J. Immunol.* 1986. *136:* 1927.
19 Leo, O., Foo, M., Sachs, D. H., Samelson, L. E. and Bluestone, J. A., *Proc. Natl. Acad. Sci. USA* 1987. *84:* 1374.
20 Lemke, H., Hämmerling, G. H. and Hämmerling, U., *Immunol. Rev.* 1979. *47:* 175.
21 Laemmli, U. K., *Nature* 1970. *277:* 680.
22 Pena-Rodriguez, A. and Rozengurt, E., *Biochem. Biophys. Res. Commun.* 1984. *120:* 1053.
23 Boyer, C., Auphan, N., Gabert, J., Blanc, D., Malissen, B. and Schmitt-Verhulst, A.-M., *J. Immunol.* 1989. *143:* 1905.
24 Oettgen, H. C., Pettey, C. L., Maloy, W. L. and Terhorst, C., *Nature* 1986. *310:* 272.
25 Hopkins, C. R., Gibson, A., Shipman, M. and Miller, K., *Nature* 1990. *346:* 335.
26 Machy, P., Truneh, A., Gennaro, D. and Hoffstein, S., *Nature* 1987. *328:* 724.
27 Albert, F., Hua, C., Truneh, A., Pierres, M. and Schmitt-Verhulst, A.-M., *J. Immunol.* 1985. *136:* 3649.
28 Kishimoto, A., Mikawa, K., Hashimoto, K., Yasuda, I., Tanaka, S.-I., Tominaga, M., Kuroda, T. and Nishizuka, Y., *J. Biol. Chem.* 1989. *264:* 4088.
29 Kaldy, P. and Schmitt-Verhulst, A.-M., *J. Immunol.* 1991, in press.
30 Hikada, H., Inagaki, M., Kawamoto, S. and Sasaki, Y., *Biochemistry* 1984. *23:* 5036.
31 Tamaoki, T., Nomoto, H., Takahashi, I., Kato, Y., Morimoto, M. and Tomita, F., *Biochem. Biophys. Res. Commun.* 1986. *135:* 397.
32 Dustin, M. L. and Springer, T. A., *Nature* 1989. *341:* 619.

33 Schaffar, L., Dallanegra, A., Breittmayer, J.-P., Carrel, S. and Fehlmann, M., *Cell. Immunol.* 1988. *116:* 52.
34 Press, O.W., Hansen, J. A., Farr, A. and Martin, P. J., *Cancer Res.* 1988. *48:* 2249.
35 Telerman, A., Amson, R. B., Romasco, F., Wybran, J., Galand, P. and Mosselmans, R., *Eur. J. Immunol.* 1987. *17:* 991.
36 Cantrell, D. A., Friedrich, B., Davies, A. A., Gullberg, M. and Crumpton, M. J., *J. Immunol.* 1989. *142:* 1626.
37 Lucas, S., Marais, R., Graves, J. D., Alexander, D., Parker, P. and Cantrell, D. A., *FEBS Lett.* 1990. *260:* 53.
38 Isakov, N., McMahon, P. and Altman, A., *J. Biol. Chem.* 1990. *265:* 2091.
39 Davies, A. A., Cantrell, D. A., Hexham, J. H., Parker, P. J., Rothbard, J. and Crumpton, M., *J. Biol. Chem.* 1987. *262:* 10918.
40 Alexander, D. R. and Cantrell, D. A., *Immunol. Today* 1989. *10:* 200.
41 Lin, C. R., Chen, W. S., Lazar, C. S., Carpenter, C. D., Gill, G. N., Evans, R. M. and Rosenfeld, M. G., *Cell* 1986. *44:* 839.
42 Felder, S., Miller, K. G. M., Ullrich, A., Schlessinger, J. and Hopkins, C. R., *Cell* 1990. *61:* 623.
43 Hedberg, K. K., Birrell, G. B., Habliston, D. L. and Griffith, O. H., *Exp. Cell. Res.* 1990. *188:* 199.
44 Herbert, J. M., Seban, E. and Maffrand, J. P., *Biochem. Biophys. Res. Commun.* 1990. *171:* 189.
45 Nakano, H., Kobayashi, E., Takahashi, I., Kato, Y., Morimoto, M. and Tomita, F., *J. Antibiot. (Tokyo)* 1986. *40:* 706.
46 Friedman, B., Fujiki, H. and Rosner, M. R., *Cancer Res.* 1990. *50:* 533.
47 Bornens, M., Paintrand, M. and Celati, C., *J. Cell Biol.* 1989. *109:* 1071.
48 Pfeffer, S. R., *New Biologist* 1990. *2:* 430.
49 Jing, S. Q., Spencer, T., Miller, K., Hopkins, C. and Trowbridge, I. S., *J. Cell Biol.* 1990. *110:* 283.
50 Vega, M. A. and Strominger, J. L., *Proc. Natl. Acad. Sci. USA* 1989. *86:* 2688.
51 Hua, C., Buferne, M. and Schmitt-Verhulst, A.-M., *Eur. J. Immunol.* 1985. *15:* 1029.